NUCLEAR SCIENCE AND ENGINEERING: **56**, 381-398 (1975)

Calculational Methods for Nuclear Heating—Part II: Applications to Fusion-Reactor Blankets and Shields

M. A. Abdou and C. W. Maynard

The University of Wisconsin, Nuclear Engineering Department
Madison, Wisconsin 53706

Received May 6, 1974
Revised October 11, 1974

The calculational methods developed for nuclear heating in an earlier paper are applied to fusion-reactor blankets and shields. The study shows that the nuclear heating in fusion-reactor blankets has been previously overestimated and is limited to ~16 MeV per DT neutron in the absence of beryllium or fissionable materials. Methods are also examined for increasing the energy multiplication in the blanket by maximizing the rates of exothermic reactions.

A general study of the sensitivity of the neutron energy deposition to changes in basic nuclear data is carried out: this study shows the following:

1. The (n, charged particles) reactions, in general, contribute ~30 to 50% to the neutron heating in typical fusion-reactor spectra. The data for these reactions, however, are not well known and in some cases are absent from the literature.

2. Approximating the neutron heating due to the (n, n', charged particles) reactions by that from the (n, n') part only, amounts to ignoring 80 to 90% of the heating.

3. For reference fusion-reactor spectra, a change in the average secondary neutron energy, $\bar{E}_{n',l}$, of the $^7Li(n,n'\alpha)t$ reaction results in a relative change in the neutron heating in ^7Li which is approximately one-third of that in $\bar{E}_{n',l}$.

4. The relative change in the neutron heating by elastic scattering due to a change in the angular distribution is larger than the relative change in $\overline{\cos\theta_{cm}}$. Ignoring the anisotropy of scattering can result in severely overestimated kerma factors.

5. The local energy deposition by radioactive decay is on the order of or less than 2% in most materials in typical spectra for controlled thermonuclear reactors.

I. INTRODUCTION

This paper is an extension of an earlier paper,[1] hereafter called Part I, which developed theoretical and computational algorithms for calculating nuclear heating in general and neutron fluence-to-kerma factors in particular. These results can be applied to numerous nuclear systems. In the present paper, we investigate nuclear heating and its sensitivity to nuclear data in fusion-reactor blankets and shields. The problems faced here are typical of those generally encountered in dealing with several other nuclear systems (e.g., a fission-reactor shield) which do not incorporate fissionable materials and where high-energy neutrons in the MeV range play an important role. In another paper to follow,[2] Part III, we will address ourselves to applications in radiology and neutron dosimetry.

Section II gives a brief description of fusion-

[1] M. A. ABDOU and C. W. MAYNARD, *Nucl. Sci. Eng.*, **56**, 360 (1975).

[2] M. A. ABDOU and C. W. MAYNARD, "Calculational Methods for Nuclear Heating—Part III: Applications to Human Tissues and Neutron Dosimetry" (to be submitted to *Nucl. Sci. Eng.*).

reactor blankets and shields. In Sec. III, the nuclear heating is calculated and analyzed for a typical fusion-reactor blanket and shield. Section IV is devoted to a general sensitivity study of nuclear heating to basic nuclear data. The conclusions are summarized in Sec. V.

II. BRIEF DESCRIPTION OF FUSION REACTORS

Figure 1 shows a schematic of a fusion reactor.[3] In a D-T fusion reaction, 17.6 MeV of energy is released in the form of a 14.1-MeV neutron and a 3.5-MeV alpha particle. The neutrons escape the plasma zone without interaction, and they are slowed down in a zone surrounding the plasma, called the blanket, where the kinetic energy is converted to heat through collisions. The blanket incorporates lithium in one form or another to breed tritium through the ^{6}Li $(n,\alpha)t$ and ^{7}Li $(n,n'\alpha)t$ reactions. The plasma is confined by superconducting magnets cryogenically cooled to about 4 K. Thus, an additional region, called the magnet shield or simply the shield, is required to further protect the magnet from radiation damage and to minimize the heat load to the refrigerators.

In many respects, the neutronics and photonics

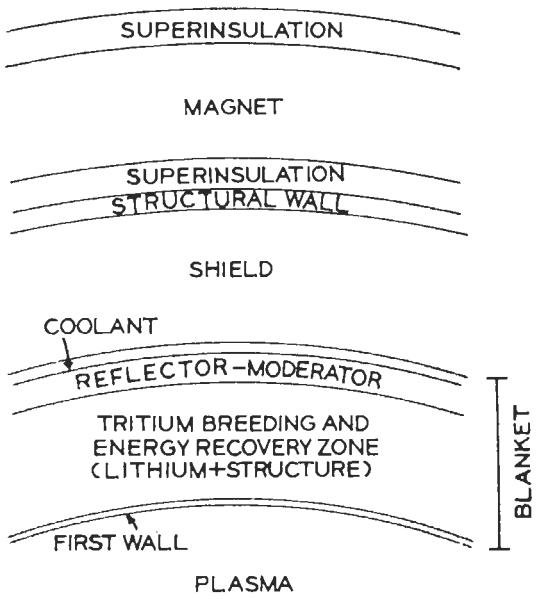

Fig. 1. Schematic of blanket and shield regions of a fusion reactor.

problems faced in the blankets and shields of a controlled thermonuclear reactor (CTR) are similar to those of any shield for a nuclear system. In the absence of fissionable materials, the calculation of the spatial distribution of nuclear heating requires the use of neutron and gamma-ray kerma factors (discussed in Part I). While we direct our attention in this paper to CTR blankets and shields, most of the discussion and conclusions are applicable, or can be extrapolated with minimum effort, to several other nuclear systems. Furthermore, most of the materials of interest in fusion reactors are those commonly used in shielding and other applications.

III. NUCLEAR HEATING IN A TYPICAL CTR

Neutron kerma factors for materials of interest in fusion reactors, shielding, and neutron dosimetry were calculated according to the methods discussed in Part I using ENDF/B-III data.[4] A documentation and description of the nuclear data in Version III of ENDF/B (e.g., reactions included, source of data, references, etc.) are given in Ref. 5. The contribution to neutron kerma factors from β^- and β^+ decay of residual nuclei of half-lives less than 50 days was added as described in Part I. The energies of the gamma rays associated with radioactive decay were excluded, as they are transported away from the site of collision and do not contribute to neutron local energy deposition. In our calculation of nuclear heating, the energies of these gamma rays were accounted for in the secondary gamma-ray source. Cross sections in both the resolved and unresolved resonance region were calculated from resonance parameters, if any, Doppler broadened at 300 K. The calculated pointwise kerma factors and group kerma factors and partial cross sections for two energy-group structures are available on magnetic tapes from the Radiation Shielding Information Center.[6]

These kerma-factor results were used to calculate the nuclear heating in a typical fusion-reactor system shown in Fig. 2. The system in cylindrical geometry consists of a central plasma region of 400-cm radius, a 50-cm-thick vacuum zone, 1-cm-thick vanadium first wall, a 40-cm-

[3]M. A. ABDOU, "Calculational Methods for Nuclear Heating and Neutronics and Photonics Design for CTR Blankets and Shields," PhD Thesis, issued as reports UWFDM-66 and UWFDM-67, University of Wisconsin (1973); also, University Microfilms, Inc., 74-8981.

[4]M. K. DRAKE, Ed., "Data Formats and Procedures for the ENDF Neutron Cross Section Library," BNL-50279, Brookhaven National Laboratory (1970).

[5]O. ÖZER and D. GARBER, "ENDF/B Summary Documentation," BNL-17541 and ENDF-201, Brookhaven National Laboratory (1973).

[6]These data can be obtained from the Radiation Shielding Information Center (as DLC-29/MACKLIB data library), Oak Ridge National Laboratory.

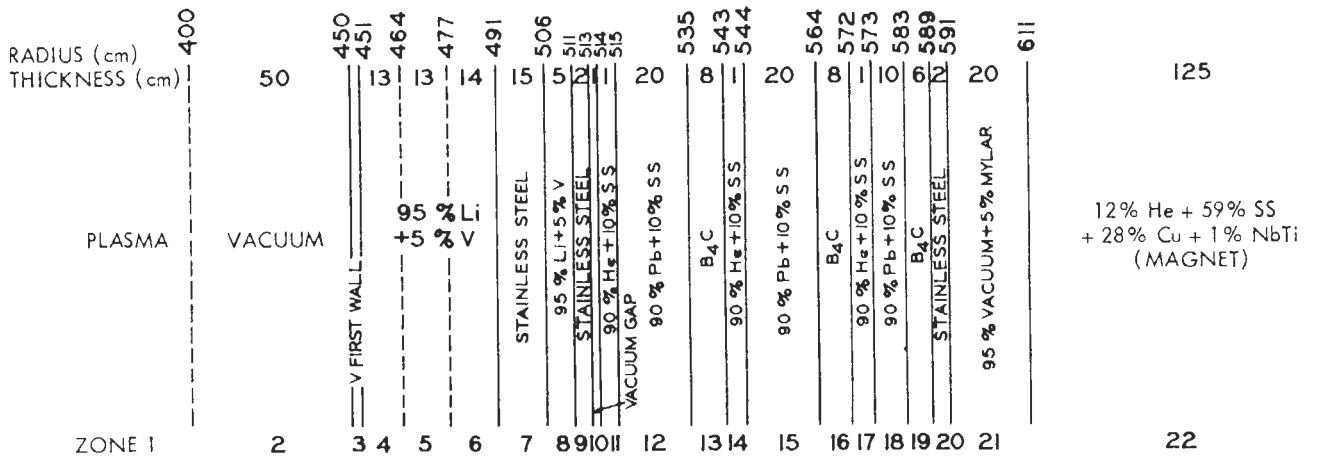

Fig. 2. A design of a CTR blanket and shield (all composition percentages by volume).

thick blanket region of 95% natural lithium plus 5% vanadium, and two stainless-steel reflector regions cooled by lithium. All composition percentages in Fig. 2 are by volume. Zones 11 through 20 represent the magnet shield, which consists of layers of boron carbide and lead with stainless steel for structural purposes and helium as the coolant. This blanket and shield design resulted from an attempt to optimize the total cost of the reactor.[3] The neutronics and photonics transport calculations were carried out in one-dimensional cylindrical geometry with the ANISN code,[7] using the S_8P_3 approximations. A uniformly distributed 14.1-MeV neutron source in the plasma region was utilized. Gamma-ray production cross sections were processed by the LAPHANO code[8] from ENDF/B-III data.

Neutron heating is given by material and zone in Table I. Neutron and gamma-ray heating and secondary gamma-ray energy production are tabulated in units of MeV per source (14.1-MeV) neutron in Table II. Several observations can be made from the results in these tables. Natural lithium contributes more than 90% to the neutron heating but only 67% to the nuclear (neutron plus gamma-ray) heating in the system. While natural lithium contains 7.56 at% ^{6}Li and 92.44 at.% ^{7}Li, the nuclear heating in ^{6}Li is roughly equal to that in ^{7}Li. This can be explained as follows: The $(n,\alpha)t$ reaction in ^{6}Li has a large cross section ($1/v$ at low energies) and is exothermic with a Q value of 4.786 MeV. About 90% of the source neutrons slow down and are absorbed in a ^{6}Li(n,α) reaction. On the other hand, all reactions in ^{7}Li except radiative capture, which has a small cross section, are endothermic; the rate of interactions in ^{7}Li, except for elastic scattering, is <60% of that in ^{6}Li.

Table II also shows that the gamma-ray energy production and heating in the light-material regions (zones 4, 5, 6, 13, 16, and 19 in Fig. 2) are much less than the neutron heating. The reverse is true for the heavy-material (lead, stainless steel, and vanadium) regions. The heavy materials are efficient in slowing the neutrons down, primarily through the inelastic reactions in which most of the energy is converted to secondary gamma rays rather than local energy deposition. Furthermore, the heavy materials have large atomic numbers and thus attenuate most of these gamma rays in addition to those streaming from neighboring light-material zones, resulting in much higher gamma-rays than neutron heating. The ratio of the neutron to gamma-ray heating can be clearly seen from Fig. 3, where the spatial distributions of neutron, gamma-ray and total heating in vanadium, lithium, and stainless-steel reflector zones are plotted. The heating rates in this figure are given in units of W/cm^3 for a neutron wall loading of 1 MW/m^2, i.e., a 14.1-MeV neutron current to the first wall of 4.43×10^{13} n/(cm^2 sec). The gamma-ray heating in the vanadium first wall (zone 3 in Fig. 2) is only about twice that of neutron heating. When vanadium is replaced by niobium, the gamma-ray heating becomes roughly ten times the neutron heating. The ratio of neutron to gamma-ray heating generally tends to decrease with increasing atomic weight.

From the results in Table II, it follows that the

[7]W. W. ENGLE, Jr., "A User's Manual for ANISN, A One-Dimensional Discrete Ordinates Transport Code with Anisotropic Scattering," K-1693, Computing Technology Center, Oak Ridge Gaseous Diffusion Plant (1967).

[8]D. J. DUDZIAK et al., "LAPHANO: A P_0 Multigroup Photon-Production Matrix and Source Code for ENDF," LA-4750-MS, Los Alamos Scientific Laboratory (1972); also, ENDF-156.

TABLE I

Neutron Heating by Material and Zone for the Design Shown in Fig. 2
(All quantities are expressed in units of MeV per source neutron.)

Zone	Composition	^{6}Li	^{7}Li	V	Fe	Cr	Ni	^{10}B	^{11}B	^{12}C	Pb	Sum by Zone
1	plasma											0.0
2	vacuum											0.0
3	V	---	---	0.219	---	---	---	---	---	---	---	0.219
4	95% Li + 5% V	1.735	3.142	0.091	---	---	---	---	---	---	---	4.968
5	95% Li + 5% V	1.492	1.711	0.050	---	---	---	---	---	---	---	3.253
6	95% Li + 5% V	1.486	0.989	0.032	---	---	---	---	---	---	---	2.507
7	SS	---	---	---	0.255	0.059	0.008	---	---	---	---	0.402
8	95% Li + 5% V	0.342	0.039	0.002	---	---	---	---	---	---	---	0.383
9	SS	---	---	---	8.04(-3)[a]	1.96(-3)	2.43(-3)	---	---	---	---	1.243(-2)
10	vacuum	---	---	---	---	---	---	---	---	---	---	0.0
11	90% He + 10% SS	---	---	---	3.57(-4)	8.75(-5)	1.05(-4)	---	---	---	---	5.49(-4)
12	90% Pb + 10% SS	---	---	---	3.67(-3)	9.11(-4)	1.01(-3)	---	---	---	7.58(-3)	1.32(-2)
13	B_4C	---	---	---	---	---	---	2.02(-1)	1.04(-2)	3.18(-2)	---	2.13(-2)
14	90% He + 10% SS	---	---	---	1.75(-5)	4.24(-6)	5.30(-6)	---	---	---	---	2.70(-5)
15	90% Pb + 10% SS	---	---	---	1.82(-4)	4.53(-5)	5.30(-5)	---	---	---	3.93(-4)	6.71(-4)
16	B_4C	---	---	---	---	---	---	9.23(-3)	5.45(-4)	1.65(-4)	---	9.94(-3)
17	90% He + 10% SS	---	---	---	8.18(-7)	2.00(-7)	2.45(-7)	---	---	---	---	1.26(-6)
18	90% Pb + 10% SS	---	---	---	5.51(-6)	1.36(-6)	1.56(-6)	---	---	---	1.16(-5)	2.85(-5)
19	B_4C	---	---	---	---	---	---	6.84(-4)	4.42(-5)	1.35(-5)	---	7.42(-4)
20	SS	---	---	---	1.95(-6)	4.71(-7)	6.07(-7)	---	---	---	---	3.03(-6)
Sum by material		5.055	5.880	0.394	0.268	0.062	0.091	0.212	0.011	0.003	0.008	11.976

[a]Read as 8.04×10^{-3}.

TABLE II

Neutron and Gamma-Ray Heating and Gamma-Ray Energy Production (in MeV per Source Neutron) by Zone for the Design Shown in Fig. 2

Zone	Composition	Neutron Heating	Gamma-Ray Energy Production	Gamma-Ray Heating	Total Heating
1	plasma	0.0	0.0	0.0	0.0
2	vacuum	0.0	0.0	0.0	0.0
3	V	0.219	0.778	0.499	0.718
4	95% Li + 5% V	4.968	0.859	0.649	5.617
5	95% Li + 5% V	3.253	0.492	0.514	3.767
6	95% Li + 5% V	2.507	0.298	0.414	2.921
7	SS	0.402	1.836	2.125	2.527
8	95% Li + 5% V	0.383	0.014	0.019	0.402
9	SS	1.243(-2)	7.44(-2)	7.16(-2)	8.40(-2)
10	vacuum	0.0	0.0	0.0	0.0
11	90% He + 10% SS	5.49(-4)	3.39(-3)	2.44(-3)	2.99(-3)
12	90% Pb + 10% SS	1.32(-2)	9.12(-2)	1.52(-1)	1.65(-1)
13	B_4C	2.13(-1)	6.45(-4)	8.18(-4)	2.13(-1)
14	90% He + 10% SS	2.70(-5)	1.22(-4)	3.92(-5)	6.62(-5)
15	90% Pb + 10% SS	6.71(-4)	3.91(-3)	4.51(-3)	5.18(-3)
16	B_4C	9.94(-3)	2.95(-5)	3.70(-5)	9.98(-3)
17	90% He + 10% SS	1.26(-6)	5.77(-6)	1.77(-6)	3.03(-6)
18	90% Pb + 10% SS	2.85(-5)	1.21(-4)	1.53(-4)	1.82(-4)
19	B_4C	7.42(-4)	3.36(-6)	7.88(-6)	7.50(-5)
20	SS	3.03(-6)	2.64(-5)	1.78(-5)	2.08(-5)
Sum for system		11.976	4.450	4.45	16.43

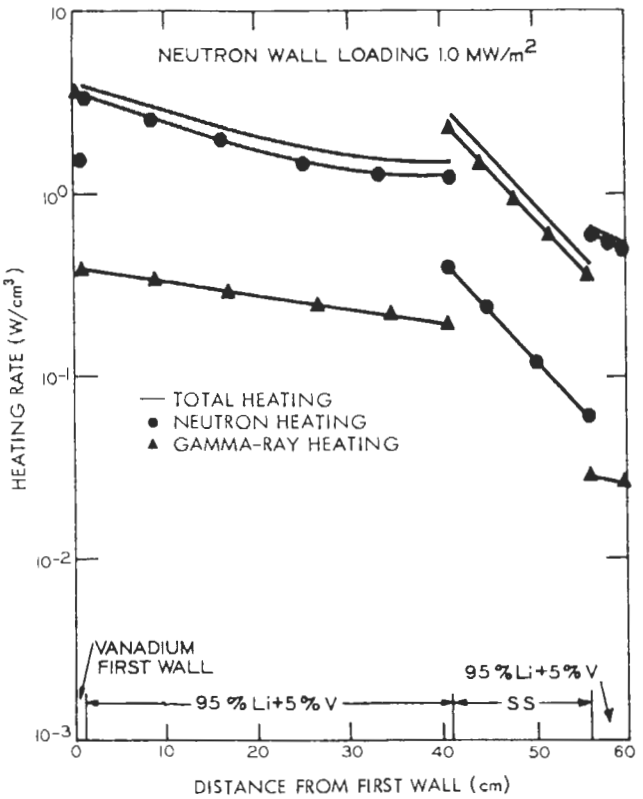

Fig. 3. Spatial distribution of heating rates in blanket and reflector regions of the design shown in Fig. 2.

nuclear heating rate in the shield (zones 11 through 20 in Fig. 2) is about 2.5% of the total nuclear heating rate in the system. Extracting this amount of energy at high efficiency is therefore not crucial from a total plant economics point of view. However, for 1 MW/m^2 neutron wall loading, the average power density in the shield is 0.35 W/cm^3, and it is necessary to remove this energy to ensure the physical integrity of the shield.

Table II shows that the total nuclear heating in the blanket and shield is 16.43 MeV, which is about 2 MeV or more less than the values reported earlier in the literature[9] for similar systems. The total recoverable energy (nuclear heating plus the 3.5-MeV kinetic energy of the alpha particle) is therefore ~20 MeV, which is an order of magnitude lower than the energy release per fission reaction. Hence, for the same thermal power, fusion reactors are required to produce far more neutrons than are fission reactors.

From an economics point of view, it is then essential in the design of CTR blankets to maximize the energy production per fusion reaction. At this time, the following options are available: (a) incorporating fissionable materials in the blanket, (b) enriching lithium in ^{6}Li to maximize the (n,α) exothermic reaction rates, and/or (c) adding beryllium to the blanket. The first option is the only one that would multiply the blanket energy production very significantly. However, allowing the long-lived radioactivity hazards associated with fission products in the blanket would negate one of the strongest motivations for developing fusion reactors. Thus, the other two options are probably the only acceptable possibilities at this time, and their effect on energy multiplication is investigated next.

The effect of enriching lithium in ^{6}Li and adding beryllium was investigated for the blanket (zones 3 through 10) of Fig. 2, except that the angular quadrature in the neutron and gamma-ray transport calculations was approximated by S_4. The neutron and gamma-ray heating, as well as the tritium breeding ratio (number of tritium atoms produced per fusion reaction), are shown in Table III for 7.42, 15, 30, and 50 at.% enriched lithium and for additional 9 and 20 vol% beryllium. The results show that the gain in energy multiplication as the ^{6}Li isotopic ratio is increased is only 0.09% for 15% ^{6}Li, and 0.5% for 50% ^{6}Li. However, adding 4 and 10 cm of beryllium to the blanket increases the energy production by about 9 and 18%, respectively. The reason the increase in energy multiplication is small when lithium is enriched in ^{6}Li can be seen from Table IV, which summarizes the rates of exothermic and endothermic reactions in ^{6}Li and ^{7}Li. The reaction rates are compared in this table for the two cases of natural lithium (7.42 at.% ^{6}Li) and a 30.0% ^{6}Li abundance in lithium. An increase in the ^{6}Li(n,α) reaction rate by 0.1487 reactions per fusion neutron corresponds to a net gain of 0.7117 MeV. The $(n,n'd)$ and $(n,2n)$ high-energy reactions in ^{6}Li are endothermic; increasing the ^{6}Li isotopic ratio in lithium results in an energy "loss" through these reactions. The net gain in ^{6}Li is 0.31 MeV. As mentioned earlier, all reactions in ^{7}Li, except radiative capture which has a small cross section, are endothermic. Decreasing the ^{7}Li isotopic ratio from 92.58 to 70 at.% reduces the energy loss and hence corresponds to a net gain of 0.48 MeV. In addition, increasing the ^{6}Li isotopic ratio in lithium hardens the spectrum and enhances the high-energy endothermic reactions in vanadium, iron, chromium, and nickel, resulting in a loss in the blanket energy production. Thus, increasing the isotopic ratio of ^{6}Li in lithium in typical fusion blankets does not improve the economy. On the other hand, adding beryllium to the

[9] M. A. ABDOU and R. W. CONN, *Trans. Am. Nucl. Soc.*, **18**, 22 (1974).

TABLE III

Effect of Enriching Lithium in Lithium-6 and of Adding Beryllium on the Energy Multiplication in the Blanket (The results are normalized to one fusion neutron.)

at.% of ^{6}Li in lithium	7.42[a]	15.0	30.0	50.0	7.42[a]	7.42[a]
vol% of beryllium in the blanket	0.0	0.0	0.0	0.0	9	20
Neutron heating (MeV) in						
^{6}Li	4.9966	6.1338	7.6839	9.3943	6.4462	7.9520
^{7}Li	6.0376	5.4082	4.3270	2.9924	4.7795	3.5067
vanadium	0.3953	0.3750	0.3590	0.3481	0.3756	0.3528
iron	0.2340	0.2278	0.2208	0.2153	0.1507	0.0774
nickel	0.0801	0.0785	0.0765	0.0749	0.0519	0.0269
chromium	0.0538	0.0521	0.0502	0.0487	0.0347	0.0179
beryllium	0.0	0.0	0.0	0.0	2.2193	4.3891
Total neutron heating (MeV)	11.7974	12.2754	12.7174	13.0737	14.0579	16.3497
Total gamma-ray heating (MeV)	4.2533	3.7893	3.3851	3.0627	3.4891	2.6623
Total heating (MeV)	16.0507	16.0647	16.1025	16.1364	17.5470	19.0120
Tritium breeding T_6	0.9042	0.9901	1.0529	1.0878	1.2361	1.5803
T_7	0.5547	0.5013	0.4052	0.2824	0.4410	0.3249
T	1.4589	1.4914	1.4581	1.3702	1.6771	1.9052

[a]Corresponds to natural lithium.

blanket results in a significant increase in energy multiplication. Beryllium has a large $(n,2n)$ cross section with a Q value of only -1.66 MeV. Since this Q value is less negative than high-energy reactions in most materials in the blanket, the Be$(n,2n)$ reaction increases energy multiplication by reducing the number of endothermic reactions in these materials. Furthermore, the reaction multiplies the neutrons, with both neutrons emerging at low energy where they are eventually absorbed in exothermic ^{6}Li(n,α) reactions.

Enriching lithium in ^{6}Li to ~30 to 50 at.% in the presence of 5 to 15 vol% beryllium results in better energy multiplication than that resulting from enriching lithium in the absence of beryllium or adding beryllium to natural lithium. However, the increase in energy multiplication is again modest and results in nuclear heating of only ~19 MeV. No other material (except fissionable material) offers a better neutron multiplication with smaller energy "expense" than does beryllium. Furthermore, there is no material that has a dominant high-energy exothermic reaction, and all materials that have attractive radiative capture cross sections offset the energy production by the high-energy endothermic reactions. Hence, it is concluded that the total recoverable energy (nuclear heating plus the 3.5-MeV kinetic energy of the alpha particle) per fusion reaction is limited to ~23 MeV unless fissionable materials are incorporated into the blanket.

IV. SENSITIVITY OF NEUTRON ENERGY DEPOSITION TO NUCLEAR DATA

Since the nuclear data for many materials suffer from relatively large uncertainties, it is very important to investigate the sensitivity of the nuclear heating to variations in nuclear data. The changes in energy deposition due to changes in nuclear data depend on the sensitivity of both neutron and gamma-ray fluxes and kerma factors. The sensitivity of the kerma factor to a particular change in nuclear parameters is not necessarily the same as the sensitivity of the flux to the same change. For example, a 50% change in the (n,p) cross section for a particular material may have little effect on either the absolute magnitude or the energy dependence of the neutron spectra, while the kerma factors may suffer a 20% change. The importance of a reaction in determining the neutron flux depends mainly on the magnitude of the reaction cross section; however, for energy deposition, it is the product of the reaction cross section and the energy release per reaction that matters.

The goal of this section is to determine in general terms the importance of the various reactions and parameters in ascertaining the neutron kerma factor in the energy range from 0 to 15 MeV. This will serve two purposes. First, it will provide a rapid assessment of the adequacy of

TABLE IV

Effect of Lithium-6 Enrichment on Reaction Rates and Energy Multiplication
(The reactions rates, A and B, are in units of reactions per one fusion neutron.)

Percentage of ^{6}Li in Lithium	7.42 (natural)	30.0	Reaction Q Value	Increase in Energy Deposition
	A	B	Q(MeV)	$(B-A) \times Q$ (MeV)
Lithium-6				
$(n,2n)\alpha$	5.51566(-3)	2.37665(-2)	-3.696	-6.7455(-2)
$(n,n')d$	6.96003(-2)	2.90917(-1)	-1.471	-3.25557(-1)
(n,γ)	3.58759(-5)	3.63008(-5)	+7.252	+3.272(-6)
(n,p)	1.51516(-3)	6.30972(-3)	-2.733	-1.31035(-2)
(n,α)	9.0420(-1)	1.05291(+0)	+4.786	+7.11728(-1)
Decay term for (n,p)	1.51516(-3)	6.30972(-3)	+1.560	+7.4795(-3)
Net gain in energy deposition in ^{6}Li				+0.31309
Lithium-7				
$(n,2n)$	2.32303(-2)	1.73536(-2)	-7.252	+4.26178(-2)
$(n,2n)\alpha$	2.91689(-2)	2.19858(-2)	-8.723	+6.2658(-2)
$(n,n')\alpha t$	5.54716(-1)	4.05156(-1)	-2.466	+3.6881(-1)
(n,γ)	4.88074(-4)	8.48159(-5)	+2.032	-8.1942(-4)
(n,d)	9.30694(-3)	6.99788(-3)	-7.760	+1.7918(-2)
Decay term for (n,γ)	4.88074(-4)	8.48159(-5)	+9.310	-3.7542(-3)
Decay term for (n,d)	9.30694(-3)	6.99788(-3)	+1.560	-3.60207(-3)
Net gain in energy deposition in ^{7}Li				+0.48383
Vanadium				
$(n,2n)$	1.29632(-1)	1.2974(-1)	-11.04	-0.01192(-1)
(n,γ)	2.16129(-2)	4.60876(-3)	+7.304	-1.24198(-1)
(n,p)	9.05218(-3)	8.93991(-3)	-1.683	0.18895(-3)
(n,α)	4.45364(-3)	4.44678(-3)	-2.042	0.014(-3)
Vanadium				
(n,γ) decay	2.16129(-2)	4.60876(-3)	+1.070	-1.8094(-2)
(n,p) decay	9.051218(-3)	8.93991(-3)	+0.9340	-0.10486(-3)
(n,α) decay	4.45364(-3)	4.44678(-3)	+0.2100	-0.00144(-3)
Net gain in energy deposition in vanadium				-1.4348735(-1)
Iron				
$(n,2n)$	1.2884(-2)	1.31215(-2)	-11.20	-0.266(-2)
(n,γ)	6.54436(-2)	2.44105(-2)	+7.803	-3.201813(-1)
(n,p)	8.16713(-3)	8.09318(-3)	-2.731	0.2019(-3)
(n,α)	3.92790(-3)	3.94955(-3)	-3.926	-0.08499(-3)
Decay term for (n,p)	8.16713(-3)	8.09318(-3)	0.731	0.05405(-3)
Net gain in energy deposition in iron				-3.22778(-1)

given nuclear data in determining the neutron kerma factors and heating in a particular material. Second, a knowledge of the importance of the various nuclear parameters throughout the energy range of interest will provide a basis for drawing conclusions about the degree of accuracy to which these parameters should be known.

Inspection of the neutron kinematics equations given in Part I shows that the input parameters for calculating the neutron kerma factors are as follows:

1. reaction cross sections
2. energy distribution of secondary particles

3. angular distribution of secondary particles

4. reaction Q values.

In addition, the multigroup representation requires the use of a heating rate-preserving weighting function. The neutron kerma factor, k_{ni}, for reaction i at an energy E can be written as

$$k_{ni}(E) = \sigma_i(E)\, E_{Ri} \quad , \tag{1}$$

where σ and E_R are the cross section and energy release per reaction, respectively. Hence, the change, δk_{ni}, in k_{ni} due to a change, $\delta\sigma_i$, in the cross section is directly proportional to $\delta\sigma_i$. The change in k_{ni} due to a change in the input parameters for E_R is more involved and can be derived from the kinematics equations given in Part I.

IV.A. Importance of Various Reactions

IV.A.1. Importance to Kerma Factors

To find out quantitatively the importance of the various reactions in determining the neutron kerma factor, the percentage contribution of each reaction type was calculated for several basic materials. Tables V through XII present the percentage contribution of each of the seven reaction kinematic types to the neutron kerma factor for some important CTR materials. Although these calculations are based on the neutron kerma factors calculated from specific nuclear data (ENDF/B-III), almost all these evaluations are complete enough and the data are adequate to allow general data-independent conclusions to be drawn about the importance of the various reaction types.

Tables V through XII show that the (n, charged particles) reactions, mostly (n,α) and (n,p), generally contribute about 60% or more to the neutron kerma factor, k_n, in the energy range of 10 to 15 MeV. This is no surprise since in the (n,charged particles) reactions, all the kinetic energy of the emitted particles is deposited locally in contrast

TABLE V

Percentage Contribution of Neutron Reaction Types to Neutron Kerma Factor for Aluminum-27

Energy (MeV)	Elastic Scattering	Inelastic Scattering[a]	(n,2n)	(n,γ)	(n, charged particles)[b]
15.000	5.6500	32.07	1.560	0.023	60.680
14.000	5.9100	27.82	0.308	0.022	65.930
12.000	6.7100	22.37	0.000	0.022	70.890
10.000	8.7700	17.50	0.000	0.023	73.690
8.000	15.9300	23.45	0.000	0.023	60.580
6.000	32.8100	34.45	0.000	0.019	32.720
4.000	56.9800	37.79	0.000	0.023	5.190
2.000	89.9300	9.96	0.000	0.059	0.045
1.000	98.0900	1.75	0.000	0.150	0.000
0.500	99.4700	0.00	0.000	0.530	0.000
0.100	91.7100	0.00	0.000	8.280	0.000
0.001	4.5080	0.00	0.000	95.490	0.000
1(eV)	0.0002	0.00	0.000	99.990	0.000

[a]These are combined values of ($n,n'\gamma$), ($n,n'\alpha$), and (n,n')p reactions.

[b]These are combined values of (n,p), (n,d), (n,t), and (n,α) reactions.

TABLE VI

Percentage Contribution of Neutron Reaction Types to Neutron Kerma Factor for Vanadium

Energy (MeV)	Elastic Scattering	Inelastic Scattering	(n,2n)	(n,γ)	(n, charged particles)
15.000	12.08	6.19	20.08	0.015	61.630
14.000	13.28	10.75	16.53	0.018	59.420
12.000	16.42	28.30	4.68	0.029	50.560
10.000	19.48	41.44	0.00	0.045	39.030
8.000	24.86	49.78	0.00	0.073	25.270
6.000	34.54	52.67	0.00	0.120	12.670
4.000	50.83	45.81	0.00	0.240	3.120
2.000	68.23	30.95	0.00	0.820	0.000
1.000	85.94	12.37	0.00	1.690	0.000
0.500	89.83	6.22	0.00	3.950	0.000
0.100	37.42	0.00	0.00	62.580	0.000
0.010	60.80	0.00	0.00	39.200	0.000
0.001	0.80	0.00	0.00	99.200	0.000
1(eV)	0.00	0.00	0.00	~100.000	0.000

TABLE VII

Percentage Contribution of Neutron Reaction Types to Neutron Kerma Factor for Iron

Energy (MeV)	Elastic Scattering	Inelastic Scattering	(n,2n)	(n,γ)	(n, charged particles)[a]
15.000	4.210	5.44	5.300	0.0016	85.04
14.000	4.050	7.03	3.570	0.0017	85.34
12.000	4.240	12.30	0.549	0.0020	82.90
10.000	5.890	18.19	0.000	0.0030	75.90
8.000	9.850	30.01	0.000	0.0050	60.13
6.000	22.330	40.08	0.000	0.0090	37.57
4.000	41.060	46.77	0.000	0.0160	12.14
2.000	73.280	26.68	0.000	0.0300	0.00
1.000	91.210	8.73	0.000	0.0500	0.00
0.500	99.930	0.00	0.000	0.0670	0.00
0.100	99.860	0.00	0.000	0.1300	0.00
0.010	99.890	0.00	0.000	0.1100	0.00
0.001	97.370	0.00	0.000	2.6200	0.00
1(eV)	0.180	0.00	0.000	99.8200	0.00

[a]These values are for (n,α) and (n,p) reactions.

TABLE VIII

Percentage Contribution of Neutron Reactions Types to Neutron Kerma Factor for Nickel

Energy (MeV)	Elastic Scattering	Inelastic Scattering	$(n,2n)$	(n,γ)	$(n,n'$, charged particles)[a]	$(n$, charged particles)[b]
15.000	1.41	2.77	0.32	0.0080	28.36	67.12
14.000	1.43	2.44	0.15	0.0080	18.22	77.74
12.000	1.88	2.99	0.00	0.0098	6.16	88.95
10.000	2.57	3.67	0.00	0.0110	1.27	92.46
8.000	3.27	4.39	0.00	0.0140	0.00	92.32
6.000	4.38	5.50	0.00	0.0170	0.00	90.08
4.000	9.91	10.02	0.00	0.0300	0.00	80.03
2.000	62.74	10.97	0.00	0.1000	0.00	26.17
1.000	99.84	0.00	0.00	0.1600	0.00	0.00
0.500	99.87	0.00	0.00	0.1200	0.00	0.00
0.100	99.75	0.00	0.00	0.2400	0.00	0.00
0.010	99.11	0.00	0.00	0.8900	0.00	0.00
0.001	97.00	0.00	0.00	2.9900	0.00	0.00
1(eV)	0.13	0.00	0.00	99.8700	0.00	0.00

[a]These are values for $(n,n'p)$ reaction.
[b]These values combine the (n,p) and (n,α) reactions.

to all other reactions in which a significant fraction of the energy is carried away from the site of collision by the secondary neutrons and photons.

As a result of momentum conservation, the kinetic energy of the recoil nucleus in a radiative capture reaction is small; hence, the (n,γ) contribution to neutron heating is negligible when there are several other competing reactions. Except for light nuclei, elastic scattering is important only below the inelastic threshold and above a few electron volts.

TABLE IX

Percentage Contribution of Neutron Reaction Types to Neutron Kerma Factor for Niobium

Energy (MeV)	Elastic Scattering	Inelastic Scattering	$(n,2n)$	(n,γ)	$(n$, charged particles)[a]
15.000	6.22	12.310	21.26	0.006	60.19
14.000	6.44	14.540	18.94	0.007	60.06
12.000	7.83	21.390	14.42	0.009	56.34
10.000	10.96	36.110	4.39	0.013	48.52
8.000	17.42	50.030	0.00	0.023	32.53
6.000	25.67	60.560	0.00	0.042	13.72
4.000	31.16	65.810	0.00	0.083	2.93
2.000	57.63	42.190	0.00	0.180	0.00
1.000	91.40	8.120	0.00	0.470	0.00
0.500	99.08	0.350	0.00	0.560	0.00
0.100	98.60	0.018	0.00	1.370	0.00
0.010	89.24	0.000	0.00	10.760	0.00
0.001	18.23	0.000	0.00	81.760	0.00
1(eV)	0.23	0.000	0.00	99.760	0.00

[a]These values combine the (n,α) and (n,p) reactions.

Most materials have large inelastic cross sections at relatively high energy and consequently a large contribution to k_n. Although the total inelastic cross section increases with energy over most of the energy range from the inelastic threshold up to 15 MeV, the k_n of inelastic scattering increases slowly with energy because the fraction of

TABLE X

Percentage Contribution of Neutron Reactions Types to Neutron Kerma Factor* for Lithium-6

Energy (MeV)	Elastic Scattering	Inelastic Scattering	$(n,n')d$	$(n,2n)\alpha$	(n,α) + (n,p)[a]
15.000	16.050	0.35	57.68	13.30	12.60
14.000	16.780	0.33	58.38	11.29	13.20
12.000	18.470	0.29	59.14	7.44	14.66
10.000	20.270	0.24	59.41	3.54	16.53
8.000	24.340	0.22	55.07	0.74	19.64
6.000	27.850	0.18	46.27	0.00	25.69
4.000	33.480	0.00	30.28	0.00	36.24
2.000	26.760	0.00	0.46	0.00	72.77
1.000	12.720	0.00	0.00	0.00	87.27
0.500	8.570	0.00	0.00	0.00	91.42
0.100	0.680	0.00	0.00	0.00	99.32
0.010	0.027	0.00	0.00	0.00	99.97
0.001	0.001	0.00	0.00	0.00	99.99
1(eV)	≃0.000	0.00	0.00	0.00	100.00

*The contribution of the (n,γ) reaction is $<0.0005\%$ at all energies.
[a]The contribution of the (n,p) reaction is zero below 3.2 MeV.

TABLE XI

Percentage Contribution of Neutron Reaction Types to Neutron Kerma Factors for Lithium-7

Energy (MeV)	Elastic Scattering	Inelastic Scattering	$(n,2n)$	(n,γ)	$(n,2n)\alpha$	(n,d)	$(n,n'\alpha)t$
15.000	29.16000	7.46	1.2500	0.0030	5.600	3.04	53.48
14.000	29.78000	7.32	1.1800	0.0030	3.620	2.37	55.71
12.000	32.19000	8.18	0.9739	0.0040	0.850	1.02	56.77
10.000	34.10000	10.84	0.4900	0.0040	0.023	0.17	54.37
8.000	37.66000	14.63	0.0000	0.0045	0.000	0.00	47.70
6.000	49.13000	15.14	0.0000	0.0046	0.000	0.00	35.72
4.000	85.10000	13.66	0.0000	0.0056	0.000	0.00	1.23
2.000	89.62000	10.37	0.0000	0.0130	0.000	0.00	0.00
1.000	92.94000	7.02	0.0000	0.0260	0.000	0.00	0.00
0.500	99.93000	0.00	0.0000	0.0670	0.000	0.00	0.00
0.100	98.94000	0.00	0.0000	1.0600	0.000	0.00	0.00
0.010	73.06000	0.00	0.0000	26.9300	0.000	0.00	0.00
0.001	11.02000	0.00	0.0000	88.9700	0.000	0.00	0.00
1(eV)	0.00045	0.00	0.0000	99.9900	0.000	0.00	0.00

energy carried away by secondary photons increases as the cross sections for exciting the low-lying levels diminish.

The importance of the $(n,2n)$ reaction increases at high energy at the expense of inelastic scattering. The contribution of the $(n,2n)$ reaction to k_n in the energy range of 10 to 15 MeV depends strongly on the binding energy of the last neutron in the target nucleus. The higher the binding energy is, the smaller the cross section in this energy range, and also the smaller the energy available to the recoil nucleus.

TABLE XII

Percentage Contribution of Neutron Reaction Types to Neutron Kerma Factor for Beryllium-9

Energy (MeV)	Elastic Scattering	$(n,2n)$[a]	(n,γ)	$(n$, charged particles)
15.000	17.250	74.240	0.0039	8.50
14.000	20.070	74.050	0.0041	5.87
12.000	24.370	68.860	0.0042	6.75
10.000	28.370	62.690	0.0043	8.92
8.000	30.260	57.600	0.0039	12.13
6.000	32.900	48.050	0.0034	19.03
4.000	43.230	28.390	0.0027	28.36
2.000	80.190	0.024	0.0029	19.77
1.000	98.740	0.000	0.0020	1.25
0.500	99.998	0.000	0.0017	0.00
0.100	99.990	0.000	0.0012	0.00
0.010	99.990	0.000	0.0031	0.00
0.001	99.970	0.000	0.0240	0.00
1(eV)	23.500	0.000	76.4900	0.00

[a]These values combine all modes for which there are two neutrons and two alpha particles in the exit channel.

Lithium-6, ^{7}Li, ^{9}Be, and ^{10}B are peculiar materials. As in all light nuclei, elastic scattering is an important mechanism for energy deposition in these materials. However, k_n is influenced equally or more by other reactions which have particularly large cross sections in these materials. In ^{6}Li, k_n below 1 MeV results mostly from the (n,α) reactions; at ~4.5 MeV, k_n is equally partitioned among the (n,α), elastic, and $(n,n')d$ reactions; above 7 MeV, the $(n,n')d$ contribution is >50%. In ^{7}Li, about 50% of k_n comes from the $(n,n'\alpha)t$ reaction above 8 MeV, with elastic scattering playing a more important role than in ^{6}Li. In ^{9}Be, the final products of the nonelastic (non-loss) reactions are two neutrons plus two alpha particles. The combined contribution to k_n from these modes is included in Table XII under the $(n,2n)$ reaction type and is about 30 to 50% from 3 to 6 MeV, and 50 to 75% of the total at higher energies. In ^{10}B, k_n below about 0.5 MeV is essentially from the (n,α) reaction. From 0.5 to 10 MeV, about 20% of k_n comes from elastic scattering, with the rest from the $(n$, charged particles) reactions; at higher energies, local energy deposition from inelastic scattering increases from 10% at 10 MeV to 20% at 15 MeV.

The important conclusion from Tables V through XII and the analysis of the results for several other materials is that about 50% of the neutron heating by neutrons in the energy range of 10 to 15 MeV generally results from the charged-particle-producing reactions. In materials such as stainless steel, this contribution is >70%. The importance of these reactions to energy deposition in some materials extends to lower energies depending on the reaction thresholds and the competition of other reactions. The (n,γ) is important

only below a few tens of electron volts, and the magnitude of its kerma factor depends largely on the radioactive decay (β^-) of the recoil nucleus in some materials. The importance of other types of reactions varies from one material to another.

IV. A. 2. Spectrum Effect

Since the $(n,2n)$, $(n$, charged particles), and $(n,n'$, charged particles) reactions occur generally at high energy, the importance of their contribution to k_n is weighted by the fraction of the spectrum in the high-energy range. To see the effect of this, consider two reference spectra for a CTR blanket and shield. The first is the first-wall spectrum for the system shown in Fig. 2 with a niobium first wall, and the second is an inverse energy, C/E, spectrum with C = 1.0 above 111 keV and 0.25 below. The fraction, f_0, of neutron heating generated by neutrons of energies above E_0, as a function of E_0 for the two spectra, is plotted for several CTR materials in Figs. 4 through 8. The f_0 for any E_0 varies with the position of the material in the blanket and shield but is generally bracketed by the values given for the two spectra. Note, however, that the C/E reference spectrum has a much larger fraction of neutrons below a few hundred electron volts than actually exists in all recent designs[3] of fusion systems, including that of Fig. 2.

Figure 4 shows that for the C/E spectrum, the fraction of neutron heating generated in ^{6}Li with neutrons of energies above 1 MeV is $<1\%$. Even for the first-wall spectrum whose low-energy component is largely depressed, f_0 in ^{6}Li is only 23% for an E_0 of 1 MeV. As discussed above, ^{6}Li is an unusual material because its (n,α) cross section is large at low energy. The situation is

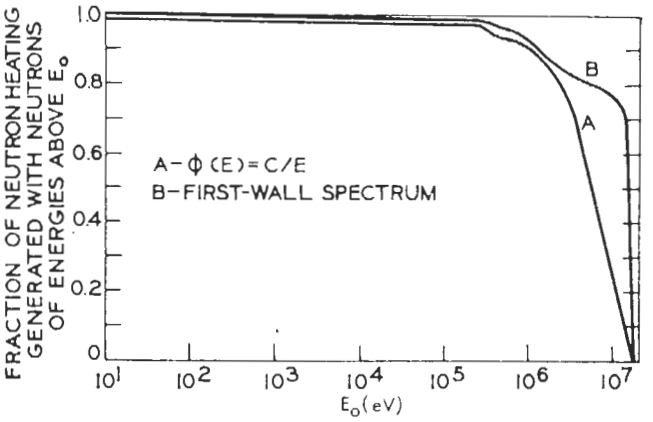

Fig. 5. Fraction of neutron heating generated in ^{7}Li with neutrons of energies above E_0, as a function of E_0 for typical CTR spectra.

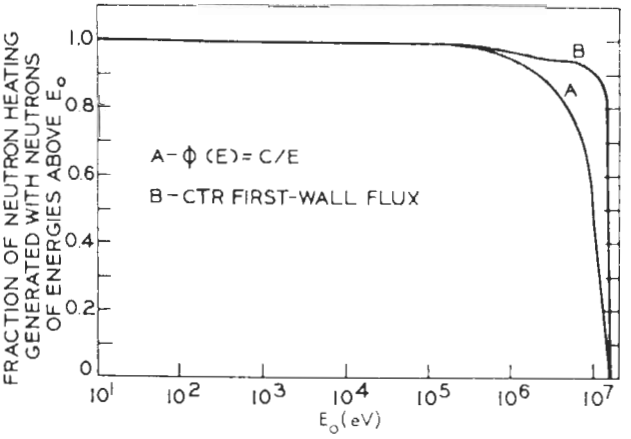

Fig. 6. Fraction of neutron heating generated in iron with neutrons of energies above E_0, as a function of E_0 for typical CTR spectra.

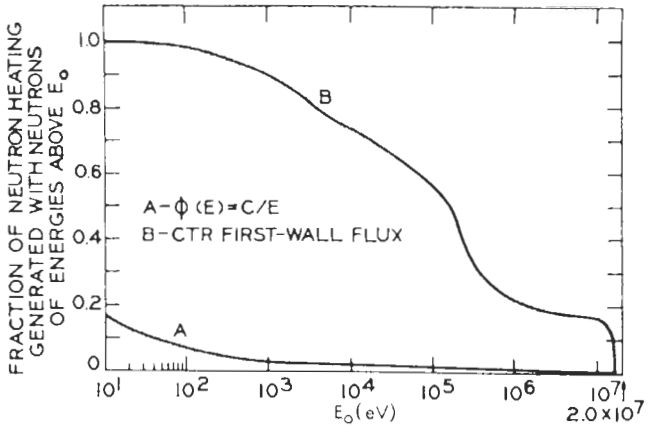

Fig. 4. Fraction of neutron heating generated in ^{6}Li with neutrons of energies above E_0, as a function of E_0 for two typical CTR spectra.

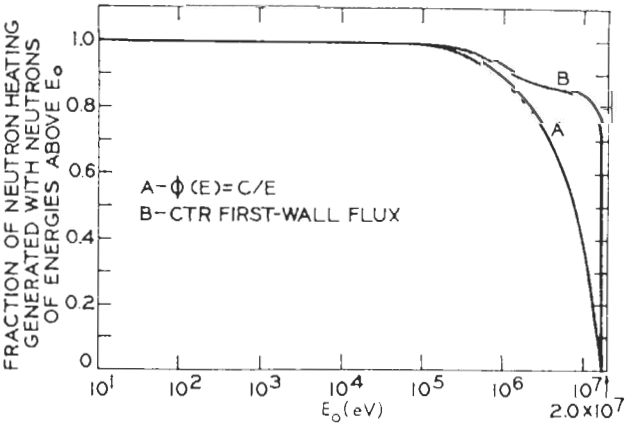

Fig. 7. Fraction of neutron heating generated in niobium with neutrons of energies above E_0, as a function of E_0 for typical CTR spectra.

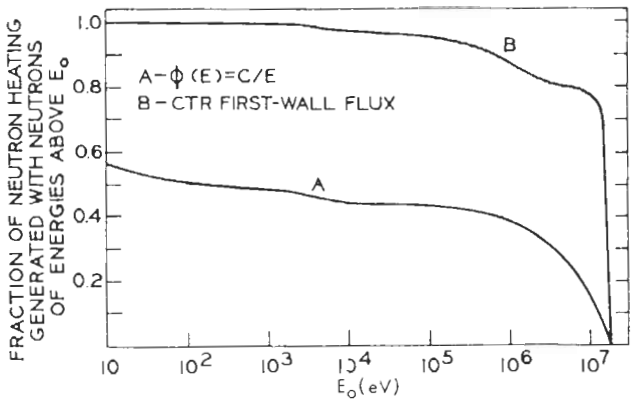

Fig. 8. Fraction of neutron heating generated in vanadium with neutrons of energies above E_0, as a function of E_0 for typical CTR spectra.

entirely different for most of the other CTR materials. Figure 6 shows that for iron about 80% of the neutron heating is generated with neutrons above 5 MeV for the C/E spectrum and that f_0 is more than 90% for an E_0 of 5 MeV in the first-wall spectrum. For materials such as Ni, Cr, Nb, and ^{23}Na, f_0 ranges from ~60 to 80% for an E_0 of 5 MeV. The k_n for vanadium is unusually large at low energy due to the (n,γ) reaction, and the fraction of neutron heating generated in vanadium with neutrons of energies above 5 MeV is only ~25% for the C/E spectrum. However, the same fraction is ~80% for the first-wall spectrum.

To derive more quantitative conclusions, the percentage contribution to neutron heating by reaction type for the two reference spectra is shown in Tables XIII and XIV for the most important CTR materials. The general conclusion from these two tables is that reactions such as (n,α) and (n,p), while relatively unimportant for determining the neutron flux, are extremely important mechanisms for neutron energy deposition. In practical systems, however, we are interested in the total nuclear heating. The ratio of neutron to gamma-ray heating in various materials was discussed in Sec. III. This ratio is often small for intermediate and heavy nuclei. These materials, in turn, generally have the highest contribution to neutron heating from charged-particle-producing reactions. Therefore, a large change in the nuclear data for charged-particle-producing reactions usually affects significantly the neutron heating, but the effect on total heating may or may not be large. For our purpose here, it suffices to say that unless the neutron heating is negligible, the contribution from the $(n,$ charged particles) reactions must be included in energy deposition calculations since it generally represents about 50% of the neutron heating.

IV.A.3. Gas-Production Data for Molybdenum

While reactions such as (n,α) and (n,p) are of prime importance in calculating energy deposition, in most materials they have little effect on the neutron spectra. In addition, there are considerable difficulties in the measurement and accurate theoretical calculation of these cross sections. Therefore, the $(n,$ charged particles) and $(n, n',$ charged particles) cross sections are generally less well known than are the other reaction cross sections for most materials. Because

TABLE XIII

Percentage Contribution of Reaction Types to Neutron Heating in Some CTR Materials for a Typical Fusion-Reactor First-Wall Spectrum

Material	Elastic Scattering	Inelastic Scattering[a]	$(n,2n)$	(n,γ)	$(n,n',$ charged particles)	$(n,$ charged particles)
^{6}Li	5.64	10.48		0.000	1.82	82.10
^{7}Li	42.20	7.78	0.089	0.040	47.32	1.77
^{9}Be	37.74		55.090[b]	0.004		7.17
^{23}Na	18.32	15.88	0.320	0.340		65.09
^{27}Al	13.95	25.74	0.350	0.250		59.70
Cr	9.84	9.88	2.260	0.030	5.53	72.46
Fe	8.84	8.21	3.270	0.010		79.65
Ni	4.33	2.82	0.140	0.010	16.92	75.74
Nb	17.57	16.35	15.520	0.090		50.46
V	24.77	12.68	12.450	3.810		46.37
Cu	12.10	11.83	4.85	30.470		40.65

[a] These values include the $(n,n',$ charged particles) contribution for some materials.

[b] The $(n,2n)\alpha$ plus $(n,n')\alpha$ plus inelastic scattering. (The final products are two neutrons and two alpha particles.)

TABLE XIV

Percentage Contribution of Reaction Types to Neutron Heating in Several CTR Materials for the Inverse Energy Spectrum

Material	Elastic Scattering	Inelastic Scattering[a]	$(n,2n)$	(n,γ)	$(n,n'$, charged particles)	$(n,$ charged particles)
^{6}Li	0.20	0.001		0.000	0.24	99.57
^{7}Li	57.71	10.86	0.26	1.840	28.97	0.36
^{9}Be	50.01		36.62[b]	0.003		13.36
^{23}Na	29.40	24.05	0.05	3.710		42.70
^{27}Al	28.64	21.34	0.06	3.060		46.89
Cr	31.03	17.46	0.62	0.090	2.04	48.76
Fe	19.71	19.44	0.99	0.030		59.79
Ni	7.97	4.56	0.03	0.030	4.46	82.94
Nb	30.58	33.31	5.82	0.220		30.07
V	18.69	13.41	1.33	56.14		10.45
Cu	9.16	8.34	22.95	3.99		55.56

[a]These values include the $(n,n'$, charged particles) contribution for some materials.
[b]The $(n,2n)\alpha$ plus $(n,n')\alpha$ plus inelastic scattering.

of this situation, the evaluations for some materials in the widely used nuclear data libraries such as ENDF/B (Ref. 4) and that of Ref. 10 do not include data for many of the possible (n, charged particles) and (n,n', charged particles) reactions. A case of interest for CTR application is the ENDF/B-III evaluation[5] for molybdenum. This evaluation does not provide information about the (n, charged particles), (n,n', charged particles) reactions, and secondary photon production. Since molybdenum is frequently proposed for use in CTR, an attempt to assess the validity of the neutron kerma factor if calculated only for the reactions in the ENDF/B-III evaluation is made next. It should be clear, however, that any reference in this work to any particular data evaluation is not by any means meant to assess the credibility of the evaluation. Rather, our purpose is to bring up important considerations in the calculation of energy deposition.

Table XV gives the abundance, Q values, and cross sections at 15 MeV for (n, charged particles) reactions in the molybdenum isotopes. These cross sections were calculated with the computer code THRESH as described in Ref. 11. Note from Table XV that the (n,α) reaction is exothermic with a relatively large Q value and that the (n,p) reaction has a relatively low threshold in all molybdenum isotopes. In the absence of information about the excitation functions to various levels, we assume here that the residual nuclei from the reactions listed in Table XV are always left in the ground state. This results in an overestimation of the neutron kerma factor from these reactions by 20 to 30%, but this is not crucial for this discussion. The last column in this table gives the neutron kerma factor for each isotope summed over all reactions given in the table. In calculating these neutron kerma factors, the contribution from radioactive decay was also added. From these results, the neutron kerma factor for natural molybdenum from charged-particle-producing reactions is 0.93 MeV b/atom. The neutron kerma factor at 15 MeV calculated from all reactions included in ENDF/B-III [elastic and inelastic scattering, $(n,2n)$, and (n,γ)] is 0.499 MeV b/atom. Even if the gamma-ray energy production in (n, charged particles) reactions is equal to (usually, it is much less than) the energy release to the recoil nucleus and charged particles emitted, the charged-particle-producing reactions contribute about 50% of the neutron heating. This is just one of several examples illustrating the strong need for new measurements and/or theoretical calculations and evaluations of the nuclear data for reactions that have a neutron in the inlet channel and one or more charged particles in the exit channel.

IV.A.4. Importance of the (n,n', charged particles) Reactions

The (n,n', charged particles) reactions generally contribute a smaller fraction to neutron heating than do the (n, charged particles) reactions because of higher thresholds and the fraction of energy carried away by the secondary neutrons.

[10]K. PARKER, "The Aldermaston Nuclear Data Library as of May 1963," AWRE 0-70/63, United Kingdom Atomic Weapons Research Establishment (1963).
[11]S. PEARLSTEIN, *J. Nucl. Energy*, **27**, 81 (1973).

TABLE XV

Abundance, Q values (in MeV), and (n, charge particles) Reaction Cross Sections (in barns) for Molybdenum Isotopes at 15 MeV

Isotope	Abundance (%)	(n,p)		(n,d)		(n,t)		$(n,{}^3\mathrm{He})$		(n,α)		k_n^a for (n, charged particles)
		Q	σ	Q	σ	Q	σ	Q	σ	Q	σ	
^{92}Mo	15.84	+0.42044	9.011(-2)	-5.2424	2.745(-2)	-11.042	2.7105(-5)	-4.9133	8.674(-4)	+3.6955	4.447(-2)	2.4979
^{94}Mo	9.04	-1.2621	4.378(-2)	-6.2661	1.435(-2)	-8.842	3.285(-3)	-6.819	3.183(-6)	+5.123	2.746(-2)	1.2996
^{95}Mo	15.72	-0.1424	3.329(-2)	-6.4104	1.169(-2)	-7.382	7.045(-3)	-7.455	5.399(-7)	+6.386	2.105(-2)	1.1002
^{96}Mo	16.53	-2.4047	2.100(-2)	-7.072	7.406(-3)	-9.3073	1.927(-3)	-8.3929	0.0	+3.968	1.515(-2)	0.6260
^{97}Mo	9.46	-1.151	1.708(-2)	-6.9962	6.624(-3)	-7.6308	4.742(-3)	-8.7366	0.0	+5.369	1.237(-2)	0.5837
^{98}Mo	23.78	-3.8193	8.923(-3)	-7.5691	4.3072(-3)	-9.3812	1.417(-3)	-9.540	0.0	+3.1988	8.416(-3)	0.3062
^{100}Mo	9.63	-5.2136	3.223(-3)	-8.3804	2.207(-3)	-9.555	9.689(-4)	---	---	+2.3975	4.532(-3)	0.1396

[a]Neutron kerma factor (in units of MeV b/atom) for (n, charged particles) at 15 MeV; the gamma-ray energies emitted in these reactions were not accounted for, but the contribution from radioactive decay of the residual nucleus is included.

However, their contribution is not negligible, and since little is known about their cross sections, some caution should be exercised in dealing with these reactions. The case encountered quite often is that in which the cross sections for the (n,n', charged particles) are combined with the inelastic scattering [$(n,n')\gamma$] reactions in the literature. Neutron kerma factors calculated from such data would then suffer from neglecting the kinetic energy of the emitted charged particles. The relative change in the energy release per reaction, E_R, from ignoring the kinetic energy of the emitted charged particles can be shown from Eqs. (10) and (21) in Part I to be

$$\frac{\delta E_R}{E_R} = \frac{-E_\lambda + |Q| + \epsilon_\gamma}{E - \bar{E}_{n',l} - |Q| - \epsilon_\gamma} \quad , \tag{2}$$

where E_λ is the energy of the level excited by the (n,n') part of the reaction and Q is the Q value for the (n,n', charged particles) reaction; ϵ_γ is the average excitation of the residual nucleus from the (n,n', charged particles) reaction and is usually smaller than E_λ, $|Q|$, and $\bar{E}_{n',l}$. In nuclides where such reactions occur, the recoil energy of the intermediate compound nucleus is small and $E - \bar{E}_{n',l}$ is only slightly greater than E_λ; hence, $\delta E_R/E_R$ is typically about 0.8 to 0.9. Therefore, combining the (n,n' charged particles) with the $(n,n')\gamma$ amounts to roughly neglecting the local energy deposition from such reactions. The effect on the total neutron heating depends, of course, on the neutron spectra as well as the relative contribution of these reactions to k_n.

As an example, consider ^{27}Al. The data for the $(n,n'\alpha)$ and $(n,n'p)$ reactions in this material are given in ENDF/B-III. The neutron heating from the $(n,n'\alpha)$ and $(n,n'p)$ in ^{27}Al is 1.35 times the neutron heating from the $(n,n')\gamma$ for a typical first-wall spectrum, but only 0.30 times as much for the C/E spectrum. The results presented in Tables XIII and XIV show that approximating the energy deposition in the $(n,n'\alpha)$ and $(n,n'p)$ in ^{27}Al by the energy deposition from the (n,n') part only results in the neutron heating being underestimated by 15% for a typical first-wall spectrum and by 5% for a typical shield spectrum. Similar results were found for vanadium, and Tables XIII and XIV show explicitly the contribution from (n,n', charged particles) in chromium and nickel. The contribution of reactions such as $(n,n'\alpha)$ and $(n,n'p)$ depends strongly on the neutron spectrum since their thresholds are particularly high in most materials.

Most of the nuclear data sets from which the neutron kerma factors in the present work were calculated did not provide information about the (n,n', charged particles) reactions. Little was found in the literature about the cross sections

and the secondary neutron energy distribution for these reactions. More information about these reactions is obviously needed. Incidentally, since the contribution from the (n,n', charged particles) to neutron heating is positive and is roughly 20 to 30% of the contribution of the (n, charged particles) reactions and since the effect of gamma-ray energy release from the (n, charged particles) on the neutron heating is negative and is also about -20 to -30% of the (n, charged particles) contribution, the neutron kerma factors calculated with the lack of both types of information are not likely to suffer from large under- or overestimations. However, this is only a qualitative statement, and there is a definite need for more information about these reactions for calculating more accurate energy deposition. Note also that these reactions are of basic importance for radiation-damage studies.

Since the energy release per reaction is independent of the reaction cross section, the change in the total neutron heating for a change, $\delta\sigma$, in the cross section with $\delta\sigma(E)/\sigma(E)$ independent of energy can be obtained directly from Tables XIII and XIV for the two reference spectra.

IV.B. Secondary Neutron Energy Distribution

The calculation of energy deposition in neutron-producing reactions requires information about the energy spectra of the secondary neutrons. The quantity of interest is the average kinetic energy, $\bar{E}_{n',l}$, of the secondary neutrons in the laboratory system.

For elastic scattering, $\bar{E}_{n',l}$ is derived from the angular distribution of the secondary neutrons. For inleastic level scattering, $\bar{E}_{n',l}$ [see Eq. (11) in Part I] is a function of the angular distribution and the energy of the excited level. The effect of changes in the angular distribution on $\bar{E}_{n',l}$ and neutron heating is studied in Sec. IV.C. For inelastic scattering into the continuum, $\bar{E}_{n',l}$ is usually derived from measured or theoretically calculated secondary neutron energy spectra. Equations (14) and (15) of Part I show that the kinetic energy of the recoil nucleus from an inelastic-scattering to continuum reaction induced by a neutron of energy E is approximately equal to $(E + \bar{E}_{n',l})/A$ for nuclides of large mass number A. Therefore, a change, $\delta E_{n',l}$, in the average energy of the secondary neutron results in a change in the neutron kerma factor, k_{nc}, for this reaction equal to $\delta E_{n',l}/A$. The relative change in k_{nc} in this case can be shown to be

$$\frac{\delta k_{nc}}{k_{nc}} = \frac{\delta E_{n',l}/\bar{E}_{n',l}}{(E/\bar{E}_{n',l}) + 1} \quad . \tag{3}$$

The ratio of E to $\bar{E}_{n',l}$ generally increases with the square root of E and A. For vanadium ($A \simeq 51$), this ratio varies from about 2.4 at 3 MeV to 4.3 at 15 MeV; and for niobium ($A \simeq 93$) and molybdenum ($A \simeq 96$), this ratio varies from about 3 at 2 MeV to 6 at 15 MeV, respectively. In structural materials in CTR blankets (intermediate- and heavy-mass nuclides), the contribution of inelastic scattering to total neutron heating is roughly 15% (see Table XIII) and comes mostly from high-energy neutrons. Thus, the relative change in neutron heating should be about 3% of the relative change in the average energy of the secondary neutron emitted in continuum inelastic scattering if the neutron flux spectrum were to remain the same. The actual change in the neutron heating is larger when changes in the neutron flux spectrum are taken into account. For light nuclides, the ratio of $E/\bar{E}_{n',l}$ is usually smaller at high energies than that for heavy nuclides, and changes in $E_{n',l}$ result in much more pronounced effects on the neutron heating, as shown next.

Approximately 80% of the neutron heating in a typical CTR blanket comes from ^{6}Li and ^{7}Li. The (n,$n'\alpha$)t reaction in ^{7}Li is the most important neutron-producing reaction in these two isotopes. Therefore, investigation of the sensitivity of the neutron heating to the secondary neutron energy distribution from this reaction is quite important.

Rosen and Stewart's data[12] for the secondary neutron energy distribution of the ^{7}Li (n,$n'\alpha$)t reaction was used as the basis for the ENDF/B-III representation. The original data were given for all but the lowest incident energies in histogram form. The ENDF/B-III evaluation has represented this secondary energy distribution with an evaporation model [see Eqs. (16) and (17) of Part I]:

$$f(E) \rightarrow E' = \frac{E'}{I} \exp[-E'/\theta(E)]$$

$$0 \leq E' \leq E - U \quad , \tag{4}$$

with U = 2.466 MeV and $\theta(E)$ given as

E	$\theta(E)$, in MeV
2.281	0.10
5.800	0.70
8.000	2.80
15.000	5.35 .

Table XVI shows that the ENDF/B-III representation consistently overestimates the average secondary neutron energy, $\bar{E}_{n',l}$, compared with the

[12] L. ROSEN and L. STEWART, "The Neutron-Induced Disintegration of ^{6}Li and ^{7}Li by 5 to 14 MeV Incident Neutrons," LA-2643, Los Alamos Scientific Laboratory (1961).

TABLE XVI

Comparison of Rosen and Stewarts (Ref. 12) and the ENDF/B-III Average Secondary Neutron Energy of the ^{7}Li $(n,n'\alpha)t$ Reaction and the Effect on Kerma Factors

Energy (MeV)	Average Secondary Neutron Energy			^{7}Li $(n,n'\alpha)t$ Kerma Factor (MeV b/atom)			^{7}Li Total Kerma Factor (MeV b/atom)		
	A_1[a]	B_1[b]	$\frac{A_1 - B_1}{B_1} \times 100$	A_2	B_2	$\frac{A_2 - B_2}{B_2} \times 100$	A_3	B_3	$\frac{A_3 - B_3}{B_3} \times 100$
5.11	1.005	0.635	58.02	0.368	0.451	-18.40	2.035	2.118	-3.920
5.62	1.191	0.811	46.85	0.675	0.806	-16.25	2.190	2.321	-5.640
6.01	1.504	0.882	70.52	0.778	1.015	-23.35	2.199	2.436	-9.730
7.03	2.354	1.512	55.69	0.927	1.281	-27.63	2.149	2.503	-14.140
8.05	3.044	2.315	31.49	1.077	1.386	-22.29	2.257	2.567	-12.076
9.03	3.543	2.748	28.93	1.264	1.597	-20.85	2.458	2.791	-11.930
10.06	4.066	3.048	33.40	1.459	1.880	-22.39	2.690	3.111	-13.530
12.00	5.041	4.285	17.64	1.707	1.994	-14.39	3.007	3.294	-7.880
13.92	6.007	4.953	21.28	1.834	2.189	-16.22	3.285	3.604	-9.750

[a]The "A" refers to data obtained using the ENDF/B-III secondary neutron energy distribution.
[b]The "B" refers to data obtained using Rosen and Stewart's secondary neutron energy distribution.[12]

Rosen and Stewart data at all incident energies. The difference is large and varies from about 20 to 60%. Why there are such large differences between the experimental and evaluated data is not the subject of this discussion; our concern here is the effect of such differences, uncertainties, or disagreements as exist in the literature on neutron heating. Table XVI shows the $(n,n'\alpha)t$ reaction and the total kerma factors for both ENDF/B-III and Rosen and Stewart data. Since Rosen and Stewart's data do not cover incident energies from threshold to 5 MeV, $E_{n',l}$ at 2.84 MeV was taken equal to that derived from ENDF/B-III data, and a linear interpolation from 2.84 to 5 MeV was assumed. Table XVI shows that the pointwise kerma factor for the $(n,n'\alpha)t$ reaction changes by ~15 to 25% and that the total kerma factor changes by 5 to 12% when the Rosen and Stewart secondary neutron energy distribution is replaced by the ENDF/B-III representation. The change in neutron heating in ^{7}Li was found to be -6.8% for the reference C/E spectrum and -8.4% for the reference first-wall spectrum; this is a relatively small change compared with the large change in $\bar{E}_{n',l}$. Note, however, that the change in $\bar{E}_{n',l}$ is ~25% in the effective range for neutron energy deposition in ^{7}Li by the $(n,n'\alpha)t$ reaction. The energy range 5 to 7 MeV, where the change in $\bar{E}_{n',l}$ is 50 to 70%, contributes little to the neutron heating by the $(n,n'\alpha)t$ reaction. Therefore, it can be concluded that the relative change in neutron heating in ^{7}Li is roughly one-third the relative change in $E_{n',l}$ for this reaction. Another study also showed that a 90% change in the nuclear temperature for all neutron-producing reactions in ^{7}Li results in a 26% change in the neutron heating for the reference shield spectrum (C/E) and 43% for the reference first-wall spectrum. Since the energy deposition in ^{7}Li by the $(n,2n)$ and $(n,2n)\alpha$ reactions is small, this result is associated with the $(n,n'\alpha)t$ reaction.

IV. C. Angular Distribution of Secondary Neutrons

Calculating neutron kerma factors requires an accurate description of the angular distribution of secondary neutrons. Since most of the nonelastic reactions are nearly isotropic in the center-of-mass, the anisotropy of the angular distribution of the secondary neutrons is most important in elastic scattering.

For intermediate and heavy nuclei, the angular distribution of elastic scattering is highly ansiotropic at high energy. For these materials, the energy deposition by elastic scattering is much smaller than the energy deposition by other reactions at high energies. This implies that small changes in the angular distribution of elastic scattering result in small changes in neutron heating in these materials. However, very large changes in the angular distribution can result in significant changes in neutron heating. The change, δk_e, in the elastic scattering kerma factor, k_e, due to a change $\delta(\overline{\cos\theta})$ in the average of the cosine of the center-of-mass scattering angle is

$$\frac{\delta k_e}{k_e} = \frac{\delta E_R}{E_R} = \frac{-\delta(\overline{\cos\theta})_{cm}}{1 - (\overline{\cos\theta})_{cm}} \quad . \tag{5}$$

TABLE XVII

Effect of Anisotropy of Elastic Scattering on Neutron Kerma Factor for Lithium-7

Energy (MeV)	Elastic-Scattering Kerma Factor			Total Kerma Factor		
	Anisotropy Included (A)	Anisotropy Ignored[a] (B)	Percentage Difference $\frac{B-A}{A}\times 100$	Anisotropy Included (C)	Anisotropy Ignored[a] (D)	Percentage Difference $\frac{D-C}{C}\times 100$
15.000	1.0122 (+6)	3.1057 (+6)	206.80	3.4713 (+6)	5.5647 (+6)	60.3
14.000	9.8342 (+5)	3.0173 (+6)	206.80	3.3016 (+6)	5.3354 (+6)	61.6
13.000	9.7673 (+5)	2.8847 (+6)	195.34	3.1358 (+6)	5.0437 (+6)	60.8
12.000	9.7132 (+5)	2.7708 (+6)	185.30	3.0174 (+6)	4.8169 (+6)	59.6
11.000	9.4591 (+5)	2.6016 (+6)	175.00	2.8652 (+6)	4.5209 (+6)	57.8
10.000	9.2003 (+5)	2.4442 (+6)	165.70	2.6904 (+6)	4.2145 (+6)	56.7
9.000	8.7611 (+5)	2.2485 (+6)	156.60	2.4584 (+6)	3.8308 (+6)	55.8
8.000	8.4998 (+5)	2.1132 (+6)	148.60	2.2571 (+6)	3.5203 (+6)	56.0
7.000	8.8583 (+5)	1.9466 (+6)	119.70	2.1489 (+6)	3.2097 (+6)	49.4
6.000	1.0894 (+6)	1.9205 (+6)	76.30	2.1991 (+6)	3.0303 (+6)	37.8
5.000	1.4101 (+6)	1.9532 (+6)	38.50	2.0073 (+6)	2.5504 (+6)	27.1
4.000	1.4599 (+6)	1.6176 (+6)	10.80	1.7131 (+6)	1.8708 (+6)	9.2
3.000	9.9446 (+5)	1.1166 (+6)	12.28	1.1257 (+6)	1.2478 (+6)	10.8
2.000	6.4237 (+5)	6.6064 (+5)	2.80	7.1680 (+5)	7.3506 (+5)	2.5
1.600	5.0763 (+5)	5.0510 (+5)	-0.50	5.6630 (+5)	5.6377 (+5)	-0.4
0.500	1.3565 (+5)	1.1782 (+5)	-13.10	1.3575 (+5)	1.1792 (+5)	-13.1
0.020	4.3930 (+3)	4.4731 (+3)	1.80	4.9644 (+3)	5.0446 (+3)	1.6
$\leq$0.009			0.00			0.0
η_s	2.7427 (+5)	4.3309 (+5)	57.9	4.7525 (+5)	6.3407 (+5)	33.4
η_w	3.3427 (+5)	7.2472 (+5)	116.8	7.9208 (+5)	1.1825 (+6)	49.3

[a]Refers to center-of-mass system.

Since $\overline{\cos\theta_{cm}}$ is typically 0.6 to 0.8 at high energies, the relative change in k_e is about three times the relative change in $\overline{\cos\theta_{cm}}$.

Since the energy range of interest extends to high energies, the anisotropy of elastic scattering in light nuclei must also be accurately described. Lithium-7 is one of the lightest nuclides in the blanket, and the effect of a 100% change in $\overline{\cos\theta_{cm}}$ for elastic scattering in this material is shown in Table XVII. The table shows that ignoring the elastic-scattering anisotropy in the center-of-mass roughly doubles the energy deposition by elastic scattering at high energies. An increase of ~50 to 60% in the total neutron kerma factor for ^{7}Li above 6 MeV results from a 100% change in $\overline{\cos\theta_{cm}}$. In Table XVII, the parameters η_s and η_w represent the neutron heating per unit fluence for the C/E and first-wall reference spectra, respectively. These parameters show that the neutron heating in ^{7}Li increases by about 33% for the reference C/E spectrum and by 49% for the reference wall spectrum. Since ~35% of the neutron heating in a natural lithium blanket comes from ^{7}Li, ignoring the center-of-mass anisotropy of elastic scattering in this material overestimates the total neutron heating by roughly 20%. Although the elastic-scattering angular distribution is more forward peaked in ^{6}Li than in ^{7}Li, ignoring the center-of-mass anisotropy of ^{6}Li elastic scattering results in a smaller change in the blanket neutron heating because the energy deposition in ^{6}Li is dominated by the (n,α) contribution.

IV. D. Contribution of Radioactive Decay

As discussed in Part I, the contribution of radioactive decay to local energy deposition by charged-particle emission needs to be added to the neutron heating. Very accurate calculations of the decay contribution to the total heating requires accounting for (a) time dependence and (b) transmutation of the radioactive residual nucleus by neutron interactions. This requires using a special-purpose program such as CINDER (Ref. 13). However, if the contribution of radioactive

[13]T. R. ENGLAND, "An Investigation of Fission Product Behavior and Decay Heating in Nuclear Reactors," PhD Thesis, University of Wisconsin (Aug. 1969).

decay is not large, this contribution can be added to the kerma factors if we assume that (a) energy deposition is negligible from radioactive residual nuclei with half-lives greater than an arbitrary cutoff, e.g., 30 days, and (b) transmutation of residual nuclei can be ignored, i.e., each residual nucleus decays before it undergoes another nuclear reaction.

Table XVIII summarizes the percentage contribution of radioactive decay to neutron heating for CTR first-wall and C/E spectra for some CTR materials. This table shows that local energy deposition by radioactive decay is less than 2% of the neutron heating in ^{6}Li, ^{7}Li, and Nb. Therefore, very accurate calculation of radioactive-decay energy deposition would only add a small correction to the total neutron heating in these materials for blanket spectra. The situation is different, however, for the case of vanadium. The decay of ^{52}V, which is produced by the ^{51}V (n,γ) reaction, contributes a very significant fraction to local energy deposition by neutrons at low energies. While this fraction is only about 7% in the first-wall spectrum, it is more than 100% in the C/E spectrum. However, since the half-life of ^{52}V is only 3.75 min, the rate of transmutation of ^{52}V by neutron interaction is quite negligible for typical CTR fluxes [10^{14} to 10^{16} n/(cm^2 sec)]. Therefore, there is little error in calculating local energy deposition from radioactive decay in vanadium by assuming a cutoff half-life of a few days and ignoring the transmutations of the residual nuclei.

TABLE XVIII

Percentage Contribution of Radioactive Decay to Neutron Heating in ^{6}Li, ^{7}Li, V, and Nb in Reference Spectra

Material	Contribution of Radioactive Decay to Neutron Heating	
	First-Wall Spectrum	C/E Spectrum
^{6}Li	0.06	0.01
^{7}Li	0.39	1.96
V	6.75	132.4
Nb	0.70	0.42

V. CONCLUSIONS

The calculational methods developed for nuclear heating in Part I were applied to fusion-reactor blankets and shields operating on the D-T cycle. A study was also made of the sensitivity of the neutron heating to changes in basic nuclear data. Most of the results are applicable, or can be extended with a minimum of effort, to other areas of the nuclear field, such as fission-reactor shields.

The study of CTR blankets showed that the total nuclear heating has been previously overestimated and is limited to ~16 MeV per DT neutron in the absence of beryllium or fissionable materials. Methods were examined for increasing the blanket energy multiplication by maximizing the rates of exothermic reactions. It was found that enriching lithium in ^{6}Li does not improve the economics of a CTR unless a neutron multiplier is present, while incorporating beryllium into the blanket does result in a significant reduction in the cost per unit power.

The sensitivity study of neutron kerma factors to changes in basic nuclear data showed the following:

1. The $(n,$ charged particles) reactions generally contribute about 30 to 50% of the neutron heating for typical fusion spectra. The data for these reactions are not well known and in some cases are absent from the literature. Thus, new evaluations, measurements, and/or theoretical calculations of these cross sections are required.

2. Approximating the neutron heating from the $(n,n'$, charged particles) reactions by that from the (n,n') part only amounts to ignoring 80 to 90% of the heating from these reactions.

3. A change in the average secondary neutron energy, $\bar{E}_{n',l}$, of the ^{7}Li$(n,n'\alpha)t$ reaction results in a relative change in the neutron heating in ^{7}Li which is approximately one-third that in $\bar{E}_{n',l}$.

4. The relative change in the neutron heating by elastic scattering due to a change in the angular distribution is larger than the relative change in $\overline{\cos\,\theta}_{cm}$. Ignoring the anisotropy of scattering can result in severely overestimated kerma factors.

5. The local energy deposition by radioactive decay is $\lesssim 2\%$ in most materials in typical CTR spectra.